Sensors and Actuators B 185 (2013) 608–619

Contents lists available at SciVerse ScienceDirect

Sensors and Actuators B: Chemical

journal homepage: www.elsevier.com/locate/snb

Facile and green fabrication of small, mono-disperse and size-controlled noble metal nanoparticles embedded in water-stable polyvinyl alcohol nanofibers: High sensitive, flexible and reliable materials for biosensors

Han Zhu [b], MingLiang Du [a,b,*], Ming Zhang [a,b], Pan Wang [b], ShiYong Bao [b], YaQin Fu [a,b], JuMing Yao [a,b]

[a] Key Laboratory of Advanced Textile Materials and Manufacturing Technology, Zhejiang Sci-Tech University, Ministry of Education, Hangzhou 310018, PR China
[b] Department of Materials Engineering, College of Materials and Textile, Zhejiang Sci-Tech University, Hangzhou 310018, PR China

ARTICLE INFO

Article history:
Received 16 February 2013
Received in revised form 12 May 2013
Accepted 16 May 2013
Available online 25 May 2013

Keywords:
Biosensor
Electrospin
Nanofiber
Nanoparticle

ABSTRACT

A facile and green approach has been demonstrated for the fabrication of highly uniform and monodisperse noble metal (Ag, Au, Pt) nanoparticles (NMNPs) in polyvinyl alcohol (PVA) nanofibers by combining an in situ reduction and electrospinning technique, which are used as efficient biosensor for the detection of H_2O_2. The small and stable NMNPs can be easily obtained in aqueous solution using EGCG as both reductant and stabilizer. Through electrospinning technique, uniform and smooth nanofibers can be obtained and the NMNPs with narrow size distributions are well dispersed in PVA nanofibers. The investigation indicates that the viscosity of the PVA solution play an important role in controlling the size of NMNPs. The fabricated AgNPs/PVA nanofibers functionalized electrodes exhibits remarkable increased electrochemical catalysis toward H_2O_2 and excellent stability and reusability. The biosensor allows the highly sensitive detection of H_2O_2 with a broad linear range span of the concentration of H_2O_2 from 10 μM to 560 μM. The rapid electrode response to the change of the H_2O_2 concentration is attributed to the fast diffusion of the H_2O_2 onto the surface of small AgNPs through the porous nanofibers structures.

1. Introduction

Noble metal nanostructures have received intensive research interests in recent decades due to their unique structure-dependent properties and potential applications in numerous fundamental and applied fields, such as catalysis, sensors, energy conversion, antibacterial, biology and biomedicine [1–4]. Recent years have witnessed tremendous efforts devoted to the design and synthesis of noble metal nanoparticles (NMNPs) in the application of electrochemical biosensors [5–7]. Electrochemical biosensors, a subclass of chemical sensors, possess high specificity of biological recognition processes [8,9]. These devices contain a biological recognition element (enzymes, proteins, antibodies, nucleic acids, cells, tissues or receptors) that selectively reacts with the target analyte and produces an electrical signal that is related to the concentration of the analyte [9,10]. Electrochemical detection of biomolecules using nanomaterials can often achieve high sensitivity because nanomaterials are extremely sensitive to electronic perturbations in the surrounding environment [11,12]. For example, Mao et al. prepared reduced graphene oxide sheet decorated with gold nanoparticles using as biosensors for the detection of protein, suggesting a lower detection limit and rapid current response [6].

It is well-known that the electrocatalytic activity of metal nanoparticles is extremely sensitive to their sizes, sharp and dispersion [13–16]. Small size usually can dramatically affect their physical and chemical properties arised from their large surface-area-to-volume ratio and the spatial confinement of electrons, phonons, and electric fields in and around these particles [17–20]. However, along with the exciting properties caused by the small size, significant challenges still remain for the preparation and isolation of nanoparticles with controlled polydispersity, toxicity, and aggregation, which are due to the high surface energy and large surface curvature of nanoparticles.

A high dispersion of NMNPs is basically important to present high catalytic activity, and unfortunately, the associated tendency of NMNPs to aggregate would lower their catalytic activity and reuse life-time [21–23]. Therefore, how to design and prepare NMNPs with long-term dispersion stability and high catalytic efficiency is a primary challenge for the widely applications. Recently, one-dimensional (1-D) nanostructures such as nanowires, nanobelts and nanotubes were used as supports to protect NMNPs against aggregating and facilitate their recovery [24,25]. Chauhan et al. fabricated Au nanoparticles/multiwalled carbon nanotubes/polymers modified Au electrodes used as lysine

* Corresponding author at: Key Laboratory of Advanced Textile Materials and Manufacturing Technology, Zhejiang Sci-Tech University, Ministry of Education, Hangzhou 310018, PR China. Tel.: +86 571 86843255.
E-mail addresses: du@zstu.edu.cn, psduml@gmail.com (M. Du).

0925-4005/$ – see front matter © 2013 Elsevier B.V. All rights reserved.
http://dx.doi.org/10.1016/j.snb.2013.05.062

biosensors, demonstrating an improved analytical performance with higher stability and low limit of detection and response time [26]. However, conventional deposition precipitation method is unlikely to produce highly dispersed NPs.

Organic polymer nanofibers have been recently recognized as a new kind of 1-D supports and besides the stabilizing and protecting effects for NMNPs, polymers can offer unique possibilities for modifying both the environment around NMNPs and access to the catalytic sites [21,22]. Through electrospinning technique, various morphologies nanofibrous mats with high specific surface area, porosity, flexibility and stability can be easily achieved [27–30]. Polyvinyl alcohol (PVA) is a water soluble polymer with good biocompatibility. Combining the flexibility, good biocompatibility and porous structures of PVA nanofibers, we use the PVA solution to prepare the uniform, well-dispersion and small size of NMNPs.

In modern life, from the viewpoint of practical applications, it would be of great value to explore a facile and green approach for the synthesis of NMNPs in nanoscience [21,31]. In our previous reports, a green reductant, tea polyphenols (TP) was used to synthesis small and uniform Au nanoparticles (AuNPs) and the TP can also act as a stabilizer for protecting the AuNPs from aggregations [31–34]. In this paper, a group of water-soluble polyphenols richly deposited in plants, epigallocatechin gallate (EGCG), was used as reductant for the synthesis of NMNPs in PVA and aqueous solution via an in situ reduction. It is easy to achieve small, highly dispersion, reliable, stable, and uniform NMNPs using this method. Through electrospinning technique, uniform and smooth nanofibers can be obtained and the NMNPs with narrow size distributions are well dispersed in PVA nanofibers. The size of AgNPs embedded in PVA nanofibers and the morphology and diameter of the nanofibers can be adjusted by changing the concentration of PVA. In order to obtain AgNPs/PVA nanofibrous mats with performance porous structures and water stability, GA vapor was used to crosslink the nanofibers. After the immersion in water for 12, 24, 48 h, respectively, the porous nanofibers structure was still well preserved, suggesting the successful crosslinkage. The functional AgNPs/PVA nanofibrous mats were used as electrochemical biosensors for the detection of H_2O_2.

2. Experiment

2.1. Materials

Silver nitrate ($AgNO_3$) was acquired from Changzhou GuoYu Environmental S&T Co., Ltd. Chloroplatinic acid ($H_2PtCl_6{\cdot}6H_2O$, 99.9%) and chloroautic acid ($HAuCl_4{\cdot}4H_2O$, 99.9%) were acquired from Shanghai Civi Chemical Technology Co., Ltd. Polyvinyl alcohol (88% hydrolyzed, Mw = 88 000), horseradish peroxidase (HRP, RZ ~ 3, activity ≥ 300 units mg^{-1}), hydroquinone (HQ) and H_2O_2 (30 wt%) were obtained from Aladdin Chemistry Co., Ltd. Epigallocatechin gallate (EGCG) was purchased from Xuancheng Baicao Plant Industry and Trade Co., Ltd. Glutaraldehyde (GA) aqueous solution (30 wt%) and phosphate buffer (PB) were obtained from Hangzhou Gaojing Fine Chemical Co., Ltd. Nafion aqueous solution (5 wt%) was obtained by Aldrich Chemistry Co., Ltd. All the chemicals were used as received without further purification. Deionized water (DIW) was used for all solution preparations.

2.2. Green synthesis of noble metal (Ag, Au, Pt) nanoparticles (NMNPs) in aqueous solution using EGCG as reductant

For the synthesis of NMNPs, 2 mL Ag (I) solution (5 mmol L^{-1}), 2 mL Au (III) solution (5.0 mmol L^{-1}) and 3 mL Pt (VI) solution (10.0 mmol L^{-1}) were firstly dissolved in 25 mL DIW under moderate stirring to get a homogeneous solution. Then, the mixture were injected into a 3-neck flask (fitted with a reflux condenser and a Teflon-coated stir bar) and heated to 65 °C with vigorously stirring by magnetic force. After a few minutes, 0.0125 g, 0.0125 g, and 0.025 g EGCG dissolved in 5 mL DIW, were injected into the above Ag (I), Au (III), and Pt (VI) solution, respectively. Samples were taken over a period time and then refrigerated at 4 °C for the following characterizations. The reaction times of each sample were 1 min, 5 min, 15 min, 30 min, 60 min, 120 and 180 min, respectively. The diameters and distribution of the NMNPs were measured by Image-Pro Plus6.2 software (200 particles of NMNPs were randomly selected for the measurement).

2.3. Preparation of NMNPs in PVA electrospun precursor solution using EGCG as reductant

5 g PVA powder was dissolved in 45 mL DIW to get a concentration of 10 wt% solution and was stirred at 80 °C for 5 h to obtain a transparent homogeneous solution. The solution was then cooled to room temperature and 10 mL 10 wt% PVA solution were injected into three 3-neck flask, respectively. The calculated amounts of $AgNO_3$ (0.0375 g), $HAuCl_4{\cdot}3H_2O$ (0.0462 g) and $H_2PtCl_6{\cdot}6H_2O$ (0.0642 g) were added into the flasks, respectively. 0.025 g EGCG dissolved in 2 mL DIW was injected into the above solutions, respectively. The solutions were kept at 65 °C under vigorously stirring for 3 h to ensure the complete reduction. After that, the precursor solutions for electrospinning were refrigerated at 4 °C for the further characterizations.

2.4. Electrospinning of NMNPs embedded in PVA nanofibers

Each of the noble-metal-PVA electrospun precursor solution was collected in a 10 ml syringe equipped with a 24 gauge stainless steel needle tip. The syringe was fixed on an electric syringe pump set to maintain a constant feed rate of 0.01 mL min^{-1}. The high voltage power supplier was connected to the needle by a high-voltage insulating wire with two clamps at the end. A grounded metal plate covered with aluminum foil served as the collector. The voltage used for electrospinning was 12 kV. The distance between the needle tip and the collector was 12 cm. All experiments were performed at room temperature. Finally, after 4 h, the NMNPs/PVA nanofibrous mats were peeled off from the aluminum foil and kept in polyethylene sealing bags. The diameters and distribution of the NMNPs and nanofibers were measured by Image-Pro Plus6.2 software (200 particles of NMNPs were randomly selected for the measurement).

2.5. Preparation of size-controlled AgNPs embedded in PVA nanofibers

1.2, 1.5 and 1.8 g PVA powder were dissolved in 13.8 13.5 and 13.2 mL DIW to get a series concentration of 8, 10, and 12 wt%, respectively. 0.0375 g $AgNO_3$ was added into the PVA solutions, respectively, and the solutions were vigorously stirred at 65 °C for 0.5 h to obtain a homogeneous solution. Then, 0.025 g EGCG dissolved in 2 mL DIW was injected into the above solutions, respectively. The solutions were kept at 65 °C under vigorously stirring for 3 h to ensure the complete reduction. After that, the precursor AgNPs/PVA solutions were used to prepare a non-woven mat via electrospinning technique. The electrospun time of the precursor solutions are 3 h and then, the AgNPs/PVA nanofiber mats were peeled off from the aluminum foil and kept in polyethylene sealing bags. The diameters and distribution of the nanofibers were measured by Image-Pro Plus6.2 software (200 nanofibers were randomly selected for the measurement).

2.6. Fabrication of the water-stable AgNPs/PVA nanofibers biosensors for H_2O_2 detection

The AgNPs/PVA nanofibers mats were firstly treated by GA vapor under vacuum oven at 80 °C for overnight to achieve the water stable nanofibers. For the fabricating procedure of the biosensor, the glassy carbon electrode (GCE) with a diameter of 3 mm was polished carefully using alumina slurry as a polisher to get a mirror-like surface, followed by rinsing with DIW and ethanol and then drying by nitrogen. The water stable AgNPs/PVA nanofibers mat was immersed in 3 mg mL^{-1} of HRP solution (1 mL) at 4 °C overnight in a humidity chamber. Then, the HRP modified AgNPs/PVA fibrous mat was glued by Nafion aqueous solution (1 wt%) on the pretreated GCE and left to dry by N_2 at room temperature. The modified electrode was washed gently with DIW and then soaked in PB at 4 °C. This modified electrode is denoted as HRP/(AgNPs/PVA)/GCE. The control sample, HRP/PVA/GCE was fabricated using similar procedures for the preparation of HRP/(AgNPs/PVA)/GCE. All the modified electrodes were stored at 4 °C in a refrigerator before further characterizations.

2.7. Biosensing experiments

Amperometric experiments were conducted with a CHI660 C workstation (Shanghai Chenhua, Shanghai). All experiments were carried out using a conventional three-electrode system in 0.1 M PB, where HRP/AgNPs/PVA/GCE was used as the working electrode, a platinum foil as the auxiliary electrode and a saturated Ag/AgCl electrode as the reference electrode. The buffer was purged with high-purity nitrogen for at least 30 min prior to each amperometric experiment, and the nitrogen environment was then kept over the solution to protect the solution from oxygen. Electrochemical performances of the fabricated electrodes were tested using a three-electrode system by cyclic voltammetry (CV).

2.8. Instrumentation

Transmission electron microscopy (TEM) images were obtained with a JSM-2100 transmission electron microscopy (JEOL, Japan) at an acceleration voltage of 200 kV. The morphologies of the electrospun NMNPs/PVA nanofibers were observed by a JSM-6700F field-emission scanning electron microscope (FE-SEM, JEOL, Japan) at an acceleration voltage of 1 kV. Fourier transform infrared (FTIR) spectra were recorded on a Nicolet 5700 FTIR spectrometer in transmittance mode at a resolution of 4 cm^{-1} and 32 scans. Ultraviolet–visible (UV–vis) spectra were obtained at 25 °C with a Lambda 900 UV-Vis spectrophotometer (Perkin Elmer, USA). X-ray photoelectron spectra of pure PVA and AgNPs/PVA nanofibers were recorded using an X-ray Photoelectron Spectrometer (Kratos Axis Ultra DLD) with an aluminum (mono) Ka source (1486.6 eV). The aluminum Ka source was operated at 15 kV and 10 mA.

3. Result and discussion

3.1. Synthesis of well-dispersed noble metal nanoparticles (NMNPs) in aqueous using EGCG as a green reductant

Due to the potential widely application of NMNPs in catalysis, sensor, bioscience, imaging and optical devices, a simple, green and stable preparation approach should draw considerable attention. In

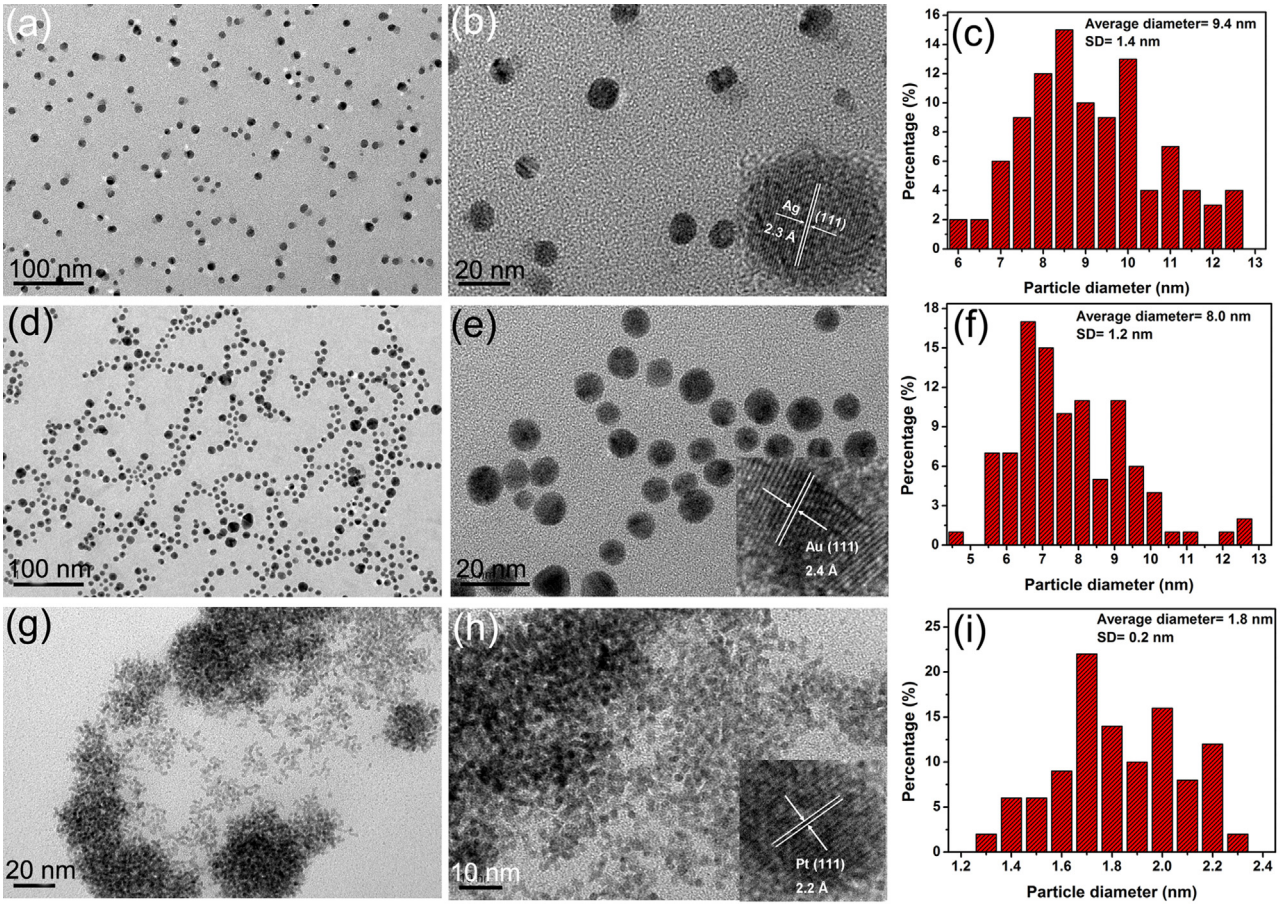

Fig. 1. TEM images of (A, B) AgNPs, (D, E) AuNPs and (G, H) PtNPs synthesized in aqueous solutions using EGCG as reductant. The corresponding diameter distributions of the (C) AgNPs, (F) AuNPs and (I) PtNPs.

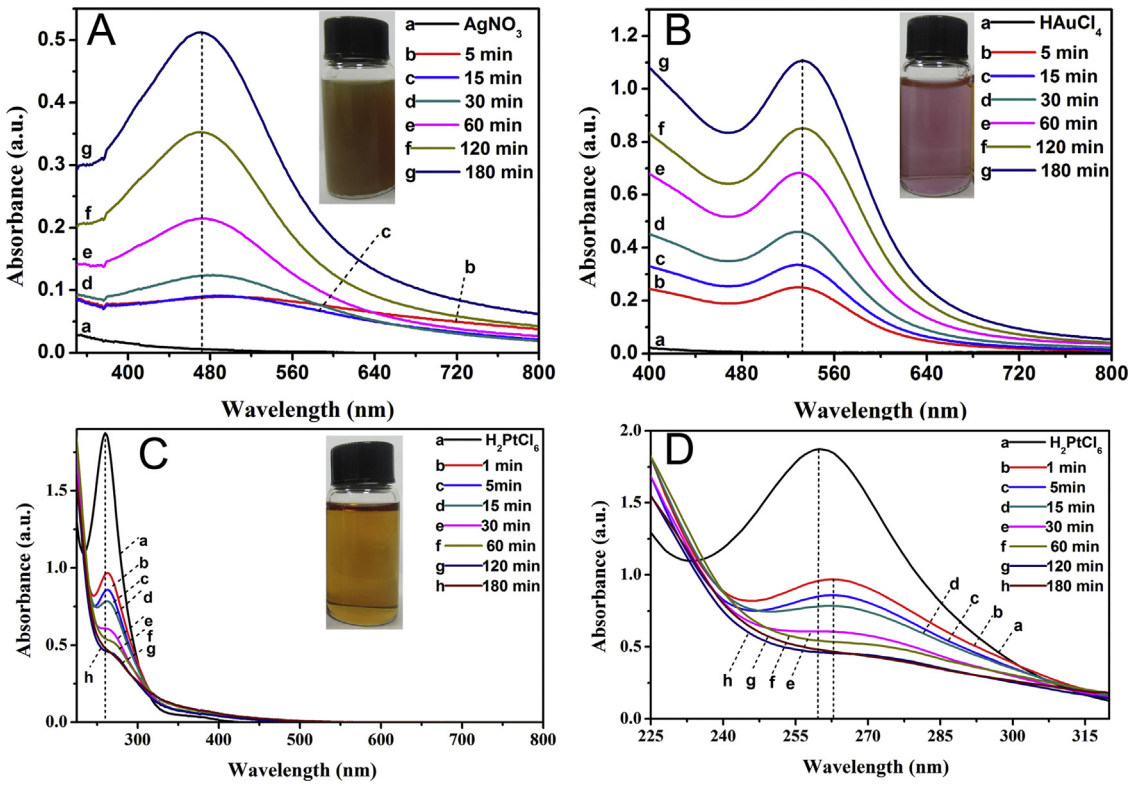

Fig. 2. UV–vis spectra of (A) AgNPs, (B) AuNPs and (C, D) PtNPs in aqueous solution and the insets are the photographs of the corresponding NMNPs solution.

the present investigation, well-dispersed and relative uniformly Ag, Au and Pt nanoparticles were obtained through a facile and green method. Fig. 1 shows the TEM and HRTEM images of the NMNPs and the corresponding diameter distributions. As exemplified in Fig. 1A and B, spherical and well-separated AgNPs are obtained and the HRTEM images shown in Fig. 1B were visible with a spacing of about 0.23 nm, which corresponded to the lattice spacing of the (1 1 1) planes of Ag [33,34]. Fig. 1C shows that the average diameter of AgNPs is 9.4 ± 1.4 nm, indicating the relative uniform diameter distribution. Meanwhile, similar phenomena are showed that there is nearly not aggregated AuNPs and PtNPs in aqueous solution, indicating the stabilization effect of polyphenols [21,33,34]. The AuNPs possess an average diameter of 8.0 ± 1.2 nm and exhibit a uniformly spherical morphology. HRTEM images exhibit the clear lattice fringes that can be assigned to Au (1 1 1) planes [35,36]. Fig. 1G and H shows the small PtNPs with a uniform diameter distribution of 1.8 ± 0.2 nm and the HRTEM images exhibit the clear lattice fringes of Pt (1 1 1) planes [23]. Based on the above results, the green reductant, EGCG, can effectively serve as a reductant and stabilizer for the synthesis of NMNPs [21,31–34].

The UV–vis spectra of the NMNPs in aqueous solution grown with increasing reaction time and the photographs of the corresponding NMNPs solution are shown in Fig. 2. The insets in Fig. 2 show that the colors of the AgNPs, AuNPs and PtNPs are brown, wine red and yellow, respectively. The color evolutions of these NMNPs solution with increasing reaction time are shown in Figs. S1, S2 and S3. Two strong surface plasmon resonance (SPR) bands corresponding to the AgNPs and AuNPs are observed, respectively, which are shown in Fig. 2A and B. They become stronger with the increasing reaction time. As shown in Fig. 2A, after the addition of EGCG, a broad band emerged around 520 nm and with the reaction time further increases, the SPR peaks of AgNPs move to 470 nm and become sharper, indicating the blue-shift of SPR peaks. As exemplified in Fig. 2B, a series of strong and sharp SPR peaks of AuNPs are observed at 525 nm, which can be considered as a superposition of the contribution from intraband transitions, and it is believed to be a consequence of photoexcitation of the free conduction electrons on the surface of AuNPs [31–34,37]. According to the literatures, the sharp SPR peaks of AgNPs and AuNPs can also indicate the relative uniformly NPs' size distribution [31–33]. Fig. 2C shows the corresponding UV–vis absorption spectra of PtNPs solution and indicates that the solution of Pt NPs has no absorption band in the visible range, which is consistent with previous reports [23]. On the other hand, Fig. 2D shows the spectra of PtNPs in the range from 225 to 315 nm. The absorption peak located at 264 nm in curve a is ascribed to $PtCl_6^{2-}$ anions and when the EGCG were added into the H_2PtCl_6 solution, the peak moves to 266 nm, which is caused by the electrostatic interactions between the $PtCl_6^{2-}$ anions and phenolic hydroxyl groups [23]. With the increasing reaction time, the peaks of $PtCl_6^{2-}$ become weak and after 3 h, the peaks are vanished, indicating the complete formation of PtNPs.

Fig. 3a shows the FTIR spectrum of EGCG, and the absorption bands at 1340 cm^{-1} and 1145 cm^{-1} are ascribed to the O—H in-plane bending vibration and to O—H aromatic, which are the characteristic peaks of EGCG. After the redox reactions in synthesizing NMNPs, the peaks at 1340 cm^{-1} and 1145 cm^{-1} become weak or vanished. Meanwhile, the absorption band around 3364 cm^{-1} shifted to 3410 cm^{-1}, 3433 cm^{-1} and 3404 cm^{-1}, respectively, and became relatively narrow, which also implied the involvement of the O—H groups in the reduction of NM ions, resulting in the partial destruction of hydrogen bonds among EGCG molecules [32–34,38]. The synthesis procedure of the NMNPs in aqueous solution is shown in Fig. S4.

3.2. *Preparation of mono-dispersed NMNPs in PVA nanofibers using EGCG as a green reductant*

In the above works, small NMNPs have been successfully synthesized using a green reducer, EGCG. However, the size control, dispersion in substrates and effective applications of these NMNPs

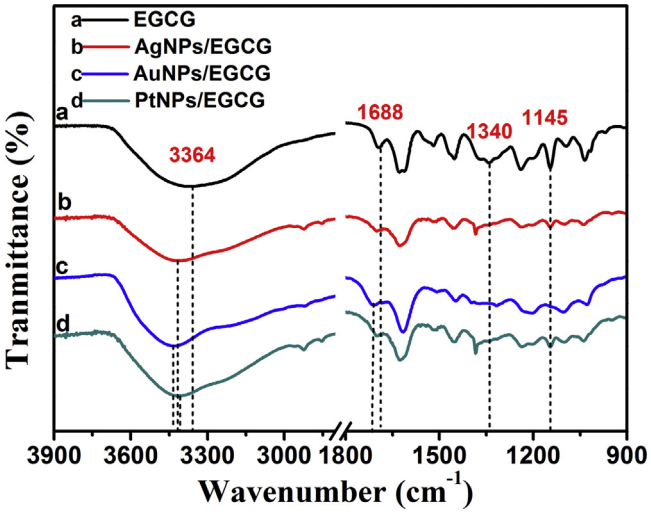

Fig. 3. FTIR spectra of (a) EGCG, (b) AgNPs/EGCG solution, (c) AuNPs/EGCG solution and (d) PtNPs/EGCG solution.

are still crucial challenges. Here, we synthesized well dispersion and stable NMNPs embedded in the PVA nanofibers by combining an in situ reduction and electrospinning technique. As shown in Fig. 4A and B, small AgNPs with an average diameter about 5.9 ± 0.5 nm are well dispersed in the PVA nanofibers. Similarly, the AuNPs and PtNPs with average diameters about 4.8 ± 0.6 and 2.6 ± 0.2 nm, respectively, are uniformly embedded in the PVA nanofibers. Compared with Fig. 1, the NMNPs embedded in PVA nanofibers had a narrow distribution and better dispersion than those in aqueous solution. Therefore, it is concluded that the PVA polymer might play a crucial role of stabilizer and direct the particular arrangements of NMNPs during the reduction and electrospinning process.

The morphologies and the diameter distributions of the NMNPs/PVA nanofibers are shown in Fig. 5. Uniform and smooth nanofibers with random orientation are obtained and the average diameters of AgNPs/PVA, AuNPs/PVA and PtNPs/PVA nanofibers are about 340 ± 45 nm, 315 ± 40 nm, and 310 ± 50 nm, respectively. A higher magnification FE-SEM image indicates that some of the NMNPs can be seen on the surface of PVA nanofibers (Fig. S5). Meanwhile, the NMNPs/PVA nanofibers indicate highly porous structure, and the porous structure can improve the adsorption of the nanofibers. The UV–vis spectra of the NMNPs/PVA solution are shown in Fig. 6A and two sharp absorption peaks located at 440 and 550 nm are the SPR bands. Compared with Fig. 2, the SPR bands of AgNPs has a hypsochromic shift from 470 nm to 440 nm, while the AuNPs has a bathochromic shift from 525 nm to 550 nm. It is well known that such hypsochromic and bathochromic shifts in the UV–vis spectra are related to chemical changes in the environment [31,39]. The UV–vis absorption spectra of PtNPs/PVA solution still have no absorption band in the visible range solution, which is consistent with Fig. 2. The FTIR spectra of PVA and NMNPs/PVA nanofibers are shown in Fig. 6B. The broaden band located around 3404 cm^{-1} are attributed to the stretching vibration of —OH groups, while the two sharp peaks at 1736 cm^{-1} and 1254 cm^{-1} are assigned to the C=O stretching vibration and C—O stretching vibration of hydroxyl groups in PVA [22,40,41]. After the fabricating of NMNPs/PVA nanofibers, the broaden band move to

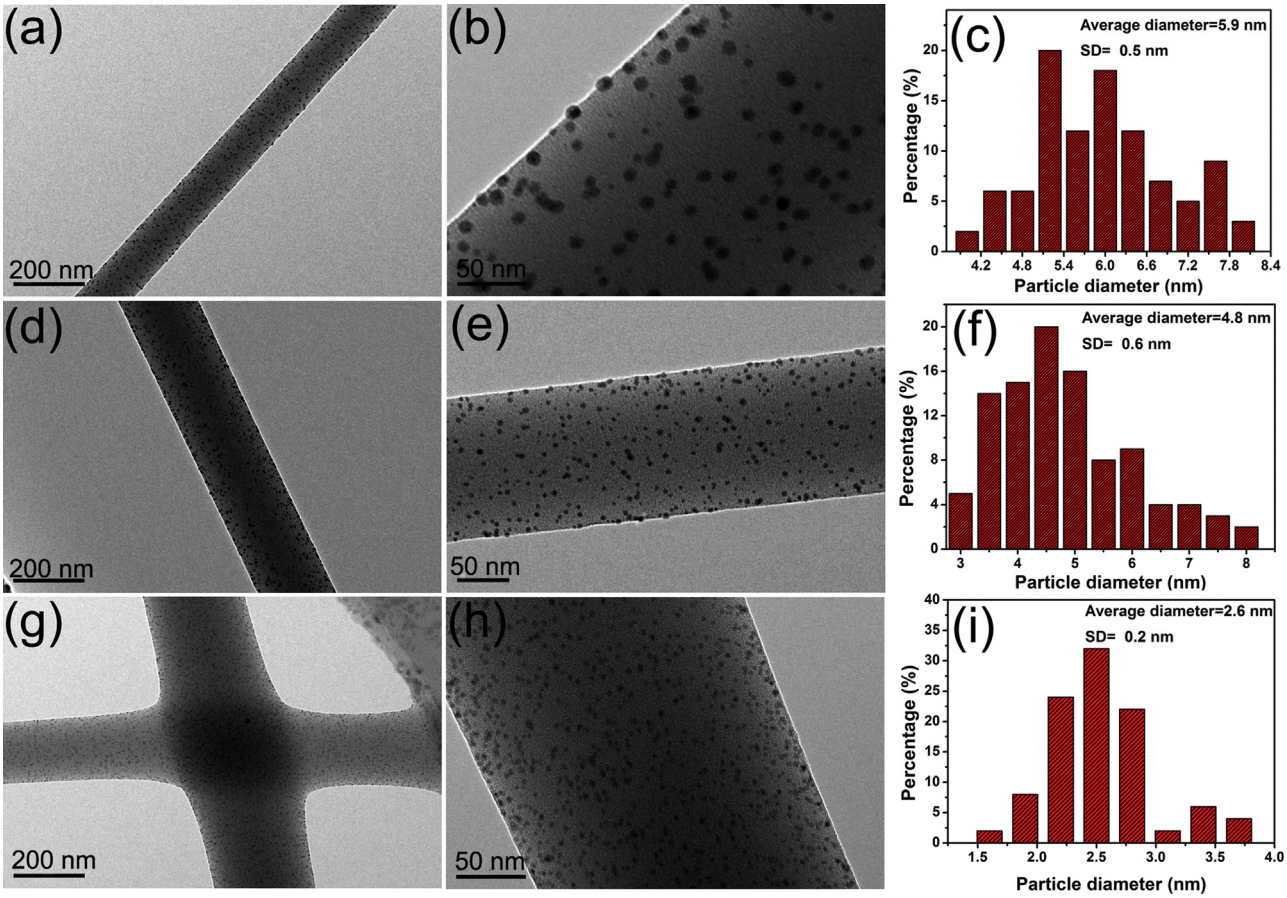

Fig. 4. TEM images of the (A, B) AgNPs/PVA, (D, E) AuNPs/PVA and (G, H) PtNPs/PVA nanofibers. The corresponding diameter distributions of (C) AgNPs, (F) AuNPs and (I) PtNPs.

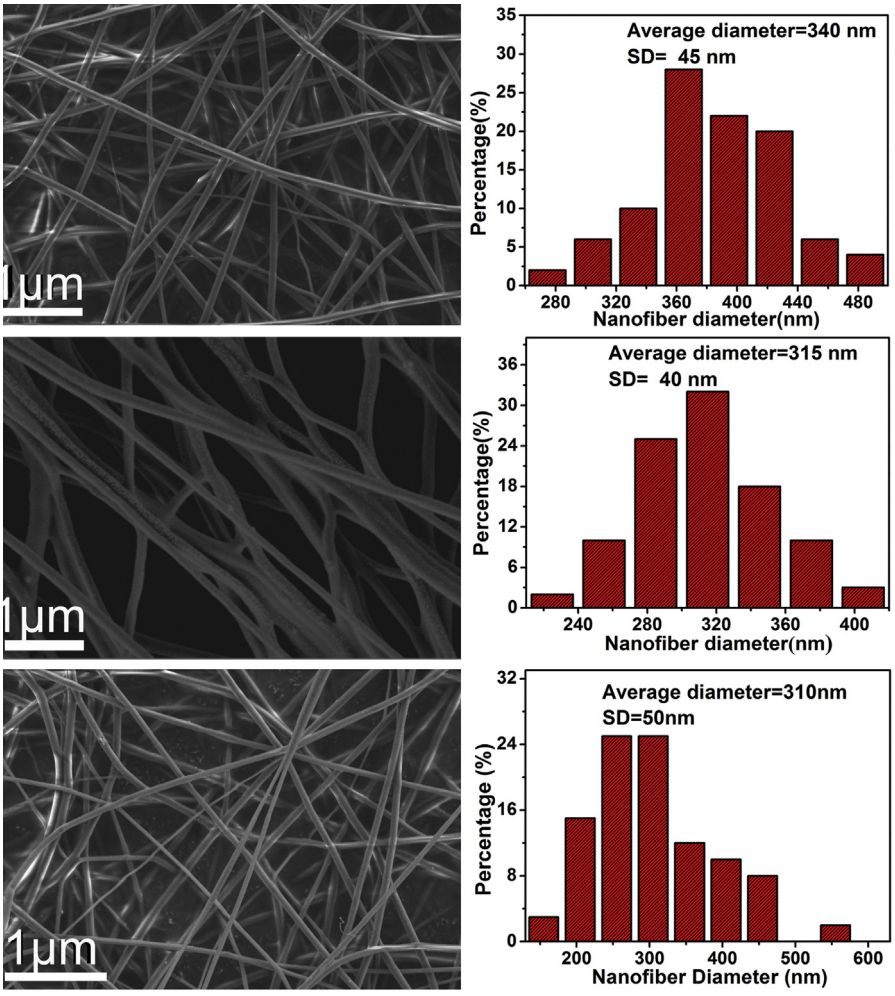

Fig. 5. FE-SEM images of the (A) AgNPs/PVA, (B) AuNPs/PVA and (C) PtNPs/PVA nanofibers with a concentration of PVA at 10 wt%. The corresponding diagrams of the average diameter of (D) AgNPs/PVA, (E) AuNPs/PVA and (F) PtNPs/PVA nanofibers.

3328 cm^{-1}, 3335 cm^{-1} and 3322 cm^{-1} respectively, suggesting the chelating effects between hydroxyls groups of PVA and NMNPs.

Based on the above studies, these novel NMNPs/PVA nanofibers have been successfully fabricated and in the following works, we will focus on the study of the growth mechanism, size control of NPs, morphologies of nanofibers, water-stability and biosensor applications. We chose AgNPs/PVA nanofibers as the example for the mentioned study. XPS was used to further probe the surface chemical compositions and chemical oxidation state of the as-prepared PVA and AgNPs/PVA nanofibers. The binding energies obtained in the XPS analysis were corrected for specimen charging by referencing the C1s to 284.6 eV. As shown in Fig. 7A, the binding energy shift of O 1s from 530.4 eV to 530.0 eV in PVA and AgNPs/PVA nanofibers was a result of the strong coordination between AgNPs and oxygen [31–34]. The XPS spectra of Ag 3d in AgNPs/PVA nanofibers demonstrates two significant peaks, locating at 371.4 and 365.7 eV, which are in agreement with the binding energies of Ag $3d_{5/2}$ and Ag $3d_{3/2}$, respectively [34,42–44]. Compared with the standard binding energy of Ag $3d_{5/2}$ and Ag $3d_{3/2}$, the binding energies of the two kind of nanofibers are lower than bulk Ag (368.2 and 374.2 eV), indicating the strong interactions among the AgNPs and hydroxyls groups. The XPS experimental data are in a good agreement with what have been reported in the reference for both Ag^+ to Ag^0 [42].

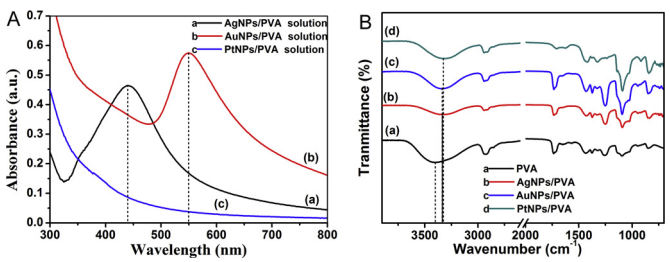

Fig. 6. (A) UV–vis spectra and (B) FTIR spectra of the AgNPs/PVA, AuNPs/PVA and PtNPs/PVA solutions.

Based on the above results, the growth mechanism of these novel materials are portrayed in Scheme 1 and the AgNPs/PVA nanofibers were taken as an example. Recently, the PVA, organic polymer, is regarded as a new class of supports for stabilizing NMNPs because in addition to stabilizing and protecting these particles, polymers can offer unique possibilities for modifying both the environment around NPs and access to the catalytic sites [21]. As illustrated in Scheme 1, the PVA molecular chains possess large amounts of hydroxyls groups, which had been proven to be excellently bonded with Ag ions by forming a stable Ag—OH chelate complex [31–34]. Because of the high viscosity of the polymer solution and the stabilization of PVA, the synthesis of AgNPs of different sizes was a kinetically driven process. After the complete formation of Ag—OH chelate complex, and with the addition of the reducer, EGCG, the pre-formed Ag—OH chelate complex were reduced to

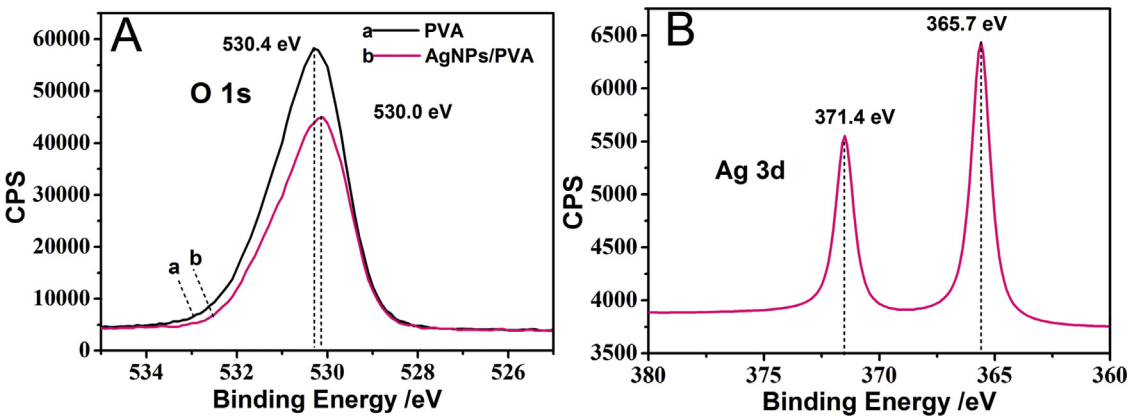

Fig. 7. XPS spectra of the PVA and AgNPs/PVA nanofibers: (A) O 1s and (B) Ag 3d spectra of PVA and AgNPs/PVA nanofibers.

the original Ag nuclei (Ag^0) in situ. Due to the high viscosity of PVA solution, the EGCG is not fast chelated with the Ag nuclei. At a relative low dosage of EGCG, the nucleation rate is relatively faster than the growth rate and more and more Ag nuclei are formed. Due to the chelating effect between the Ag ions and hydroxyls groups in PVA molecular chains, the formed Ag nuclei can be confined and cannot collide with each other to aggregate easily. When the diffusion equilibrium of EGCG is achieved, the unchelated Ag ions were coated on the surface of Ag nuclei with EGCG molecular and grown into large-sized AgNPs. Then, the synthesized AgNPs/PVA precursor solutions were electrospun into nanofibers.

3.3. *Synthesis of the size-controlled AgNPs embedded in PVA nanofibers using EGCG as a green reductant*

As discussed above, the viscosity of the PVA solution may play an important role in controlling the size of AgNPs, and therefore, we studied the effectiveness of PVA concentration on the sizes of AgNPs. The AgNPs/PVA nanofibers with different sizes of AgNPs are shown in Fig. 8. The AgNPs with various diameters are well dispersed in PVA nanofibers, indicating the reliability of this facile and green approach. With the increasing of the mass fraction of PVA from 8 wt% to 12 wt%, the average diameters of AgNPs decreased from 3.9 nm to 2.4 nm, indicating the significant effects of the viscosity on the size control. Both AgNPs achieved at different PVA's mass fractions possess narrow size distribution, and the standard deviations (SD) are 0.3, 0.3 and 0.4 nm, respectively, which are smaller than that in aqueous solution (Fig. 1).

It is well known that the uniformity of electrospun nanofibers is greatly influenced by the polymer solution properties and the electrospinning processing parameters. The morphologies of these AgNPs/PVA nanofibers with different polymer concentration (8 wt%, 10 wt%, and 12 wt%) are shown in Fig. 9. As shown in Fig. 9A, at the concentration of 8 wt%, the nanofibers possess high porous fibrous structure and the average diameter is about 260 ± 80 nm, along with some adhesion phenomenon among nanofibers. With the increasing of polymer concentration, the diameters increase from 380 nm to 410 nm. What's more, smooth and uniform nanofibers are obtained at the polymer concentration of 12 wt% (Fig. 9E). Meanwhile, the AgNPs/PVA nanofibers retain their excellent porous fiber structure and almost no adhesion phenomena occurred. The UV–vis spectra of these AgNPs/PVA precursor solutions can also provide evidences for the size-controlled AgNPs, which are shown in Fig. 10. At the same conditions, except for the polymer concentrations, a hypsochromic shifts can be obtained with the increased PVA concentration. The absorption peaks move from 438 nm to 419 nm and according to the literatures, the smaller size of NMNPs could lead to hypsochromic shifts [31–34]. The UV–vis results are according with the TEM images, which are shown in Fig. 8, indicating that the size-controlled AgNPs embedded in PVA nanofibers have been successfully fabricated by changing the polymer concentrations.

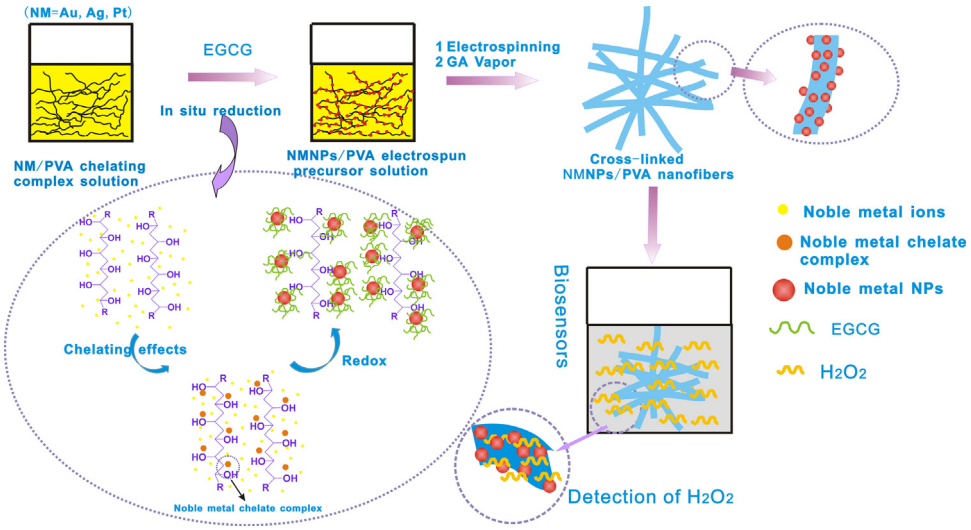

Scheme 1. A schematic illustration of the fabrication procedure of NMNPs/PVA nanofibers.

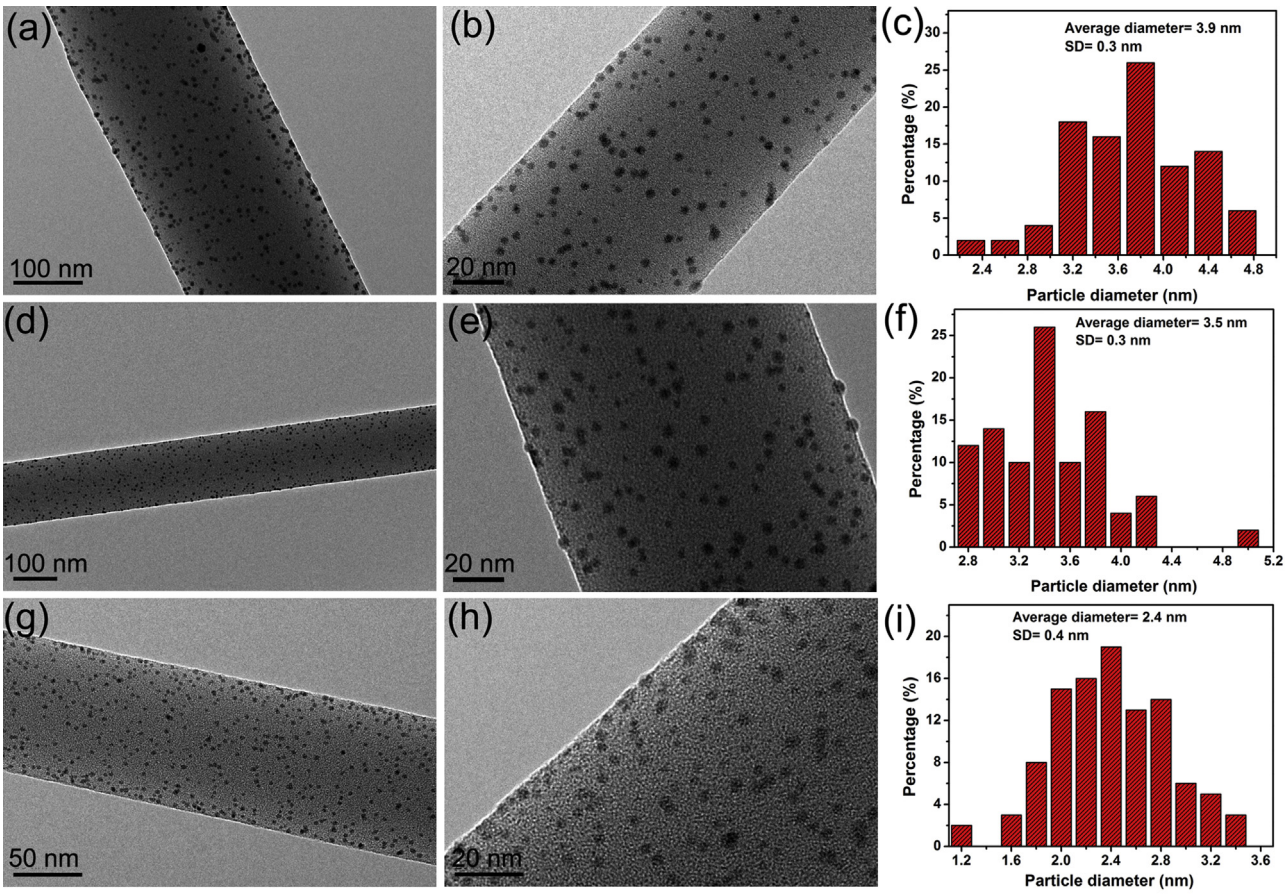

Fig. 8. TEM images of the AgNPs/PVA nanofibers with different average sizes of AgNPs by changing the mass fraction of PVA in the precursor solution: (A, B) 8 wt%, (D, E) 10 wt% and (G, H) 12 wt%. (C, F, I) The corresponding average diameters of AgNPs embedded in PVA nanofibers.

3.4. Fabrication of AgNPs/PVA nanofibers functionalized electrodes using as biosensors for the detection of H_2O_2

In the past decades, NMNPs are widely used in many areas, such as catalysis, surface enhanced Raman scattering, and antibacterial. In this paper, combining the flexibility, good biocompatibility and porous structures of PVA nanofibers with the small size, uniform and well-dispersion of NMNPs, we used these fabricated AgNPs/PVA nanofibers hybrid membranes as efficient substrate materials integrated in biosensors. As we know, the PVA used for electrospun is a kind of water-soluble polymers, and therefore, a critical problem should be solved to retain the nanofibers' water stability. In order to obtain AgNPs/PVA nanofibers with performance porous structures and water stability, GA vapor was used to crosslink the nanofibers. As shown in Fig. 11A and S5a, after the treatments with GA vapor, the nanofibers mats became water-stable and still kept excellent porous fiber structures. The average diameter of the crosslinked nanofibers (505 ± 55 nm, Fig. S5b) was larger than that of the non-crosslinked nanofibers (415 ± 40 nm, Fig. 9F), possibly due to the swelling of the nanofibers during the GA vapor crosslinking [41]. After the immersion in water for 12, 24, 48 h, respectively, the porous nanofibers structure was still well preserved (Fig. 11) and the AgNPs can clearly be seen embedded in PVA nanofibers, suggesting the successful crosslinking.

In order to broaden the application of these novel materials, the AgNPs/PVA nanofibers were used as biosensors for the detection of H_2O_2. Due to the practical applications in various fields such as food, clinical, pharmaceutical, industrial, biological, or environmental research areas, H_2O_2 detection is essential for our life and the high concentration of H_2O_2 will cause a negative effect on human health [21]. Various materials have been used as biosensors, for example, Feng et al. synthesized graphene/polyaniline composite film and the biosensor showed a good linear response over a wide range of concentrations from 1 μM to 160 μM, and a low detection limit of 0.8 μM [45]. Meanwhile, Zhong et al. prepared spherical Pd@Cys-C_{60} nanoparticles using as electrochemical biosensor for the detection of glucose [46]. Li et al. fabricated Se/Pt nanocomposites as nonenzymatic hydrogen peroxide sensor have a linear relationship with the concentration of H_2O_2 from 10 μM up to 15 mM with a correlation coefficient of 0.9991 [47]. In addition, our previous report also indicates the highly sensitive detection of H_2O_2 with a detection limit of 5 μM and exhibits a fast response, broad linear range, low detection limit and excellent stability and reusability based on the AgNPs functionalized PVA/PEI nanofibers biosensor [48]. In this paper, combining the flexibility, good biocompatibility and porous structures of PVA nanofibers with the small size, uniform and well-dispersion of NMNPs, we used these fabricated AgNPs/PVA nanofibers hybrid membranes as efficient substrate materials integrated in biosensors. For the application of enzyme-based biosensors, the electron transfer between the enzyme and the electrode is very important for the fundamental studies and the construction of biosensors [45]. Therefore, appropriate promoters should be employed to facilitate the electron transfer and retain the bioactivity of immobilized enzymes. Based on the large specific area, high conductivity, and good biocompatibility of AgNPs and porosity of the nanofibers, the horseradish peroxidase (HRP) can be easily entrapped tightly

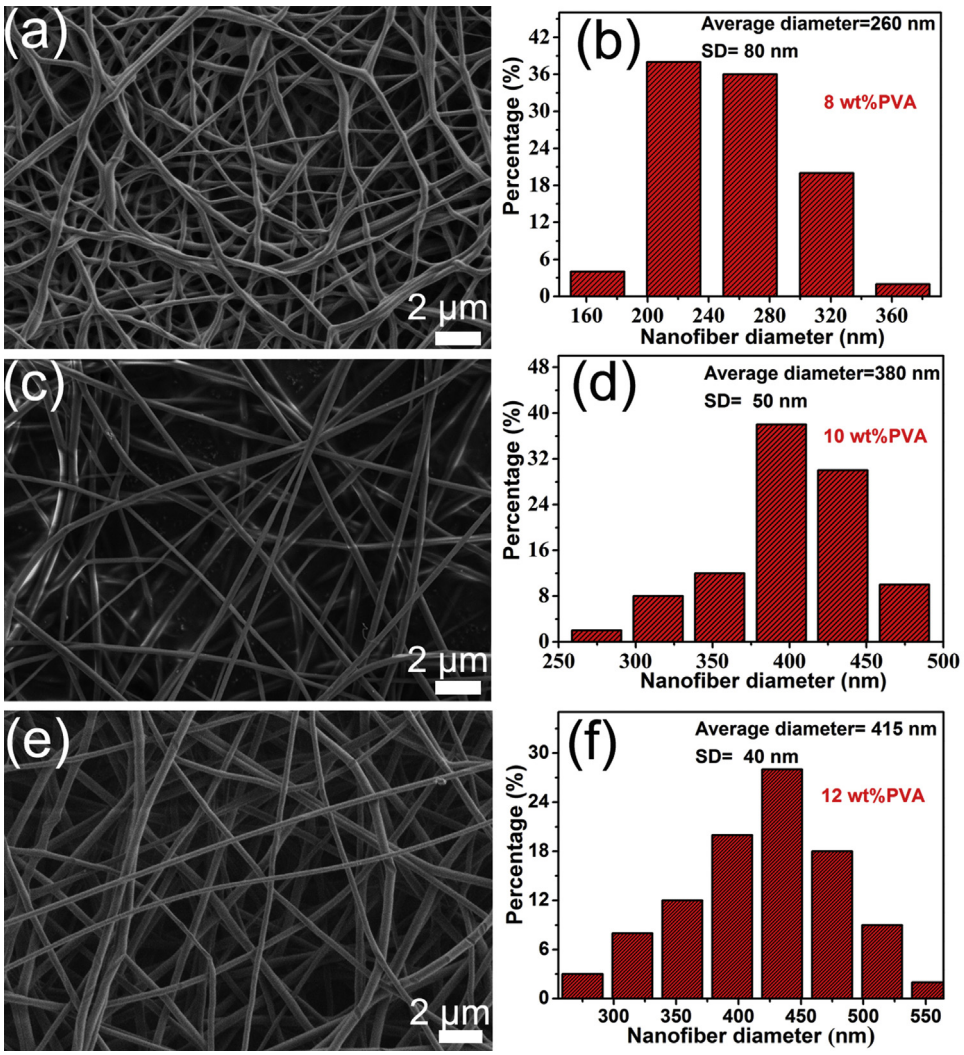

Fig. 9. FE-SEM images of AgNPs/PVA nanofibers with different PVA concentrations: (A) 8 wt%, (C) 10 wt%, and (D) 12 wt%. (B, D, F) The corresponding average diameters of the nanofibers.

onto the negatively charged AgNPs through electrostatic attraction due to its positive charge at pH values below its isoelectric point (the pH value at the isoelectric point is 8.9) [21,45]. Furthermore, hydroquinone (HQ) is used to detect hydrogen peroxide as an excellent electron mediator. The electrochemical properties of these fabricated HRP/(AgNPs/PVA)/GCE are investigated in detail, which are shown in Fig. 12. Well-defined cyclic voltammograms (CVs) of the HRP/PVA/GCE and HRP/(AgNPs/PVA)/GCE are observed with a certain concentration of H_2O_2. As shown in Fig. 12A, the HRP/PVA/GCE shows weak redox peaks with currents of HQ at 2.3 and −3.1 μA and potentials at 0.47 and −0.23 V, respectively, indicating that the PVA is not electroactive in this potential range. From Fig. 12B, the CV of HRP/(AgNPs/PVA)/GCE shows a pair of well-defined redox peaks at with currents 15.3 and −11.5 μA and potentials at 0.39 and −0.19 V, respectively. Compared with the HRP/PVA/GCE, HRP/(AgNPs/PVA)/GCE exhibits remarkable increased electrochemical catalysis toward H_2O_2, indicating the fast direct electron transfer between the redox-active site of HRP and GCE [49,50].

Apparently, the presence of the small and well-dispersed AgNPs is an important factor for the direct electron transfer of HRP [45,51,52]. Furthermore, the highly porous fibrous structure and increased surface area of AgNPs/PVA nanofibers mats also promote the electrochemical catalytic activity. As promising functional materials, the reusability and recyclability are crucial issues for practical applications, especially for the costly rare and noble metals. The fabricated AgNPs/PVA nanofibers functionalized electrodes used for 10 times were compared by the CV curves (Fig. 12B) and the redox peaks are almost the same, suggesting the

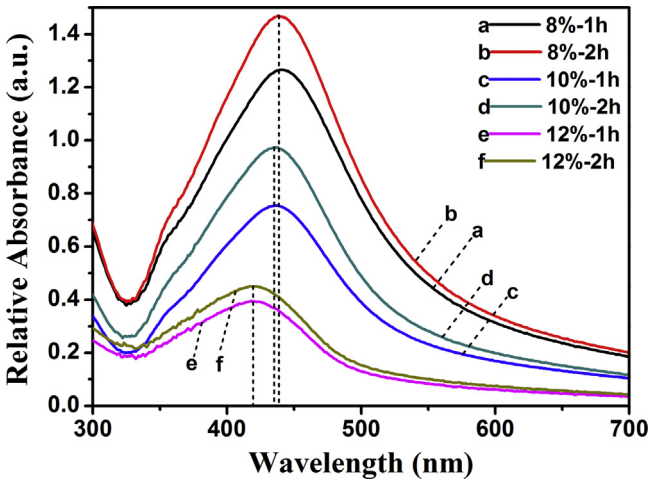

Fig. 10. UV–vis spectra of the AgNPs/PVA solutions at different PVA concentrations of 8 wt%, 10 wt% and 12 wt%.

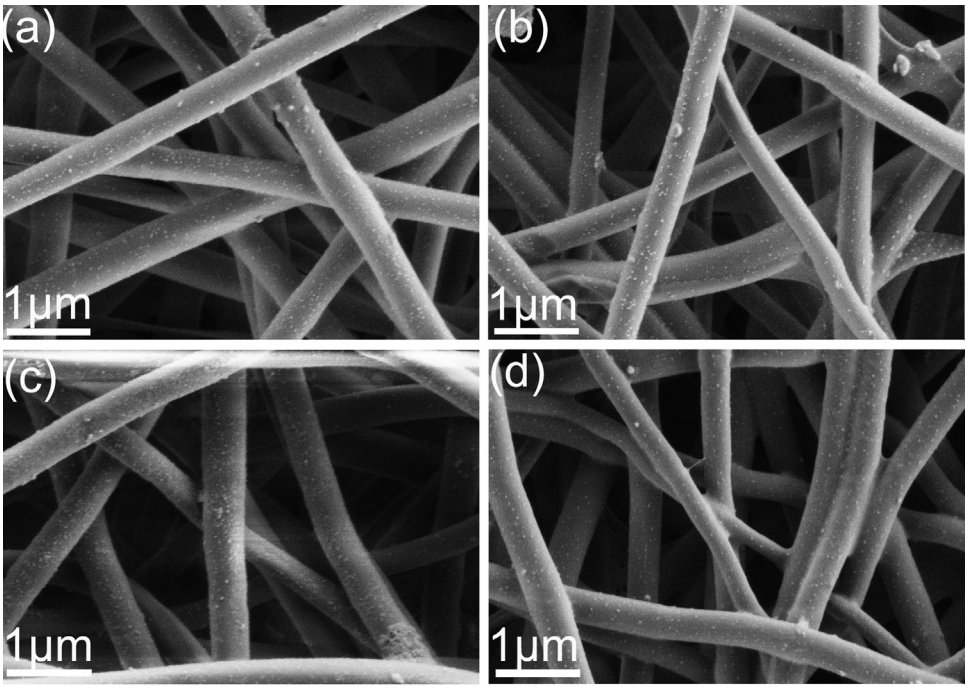

Fig. 11. FE-SEM images of (A) the cross-linked AgNPs/PVA nanofibers and different immersion time in water: (B) 12 h, (C) 24 h, and (D) 48 h.

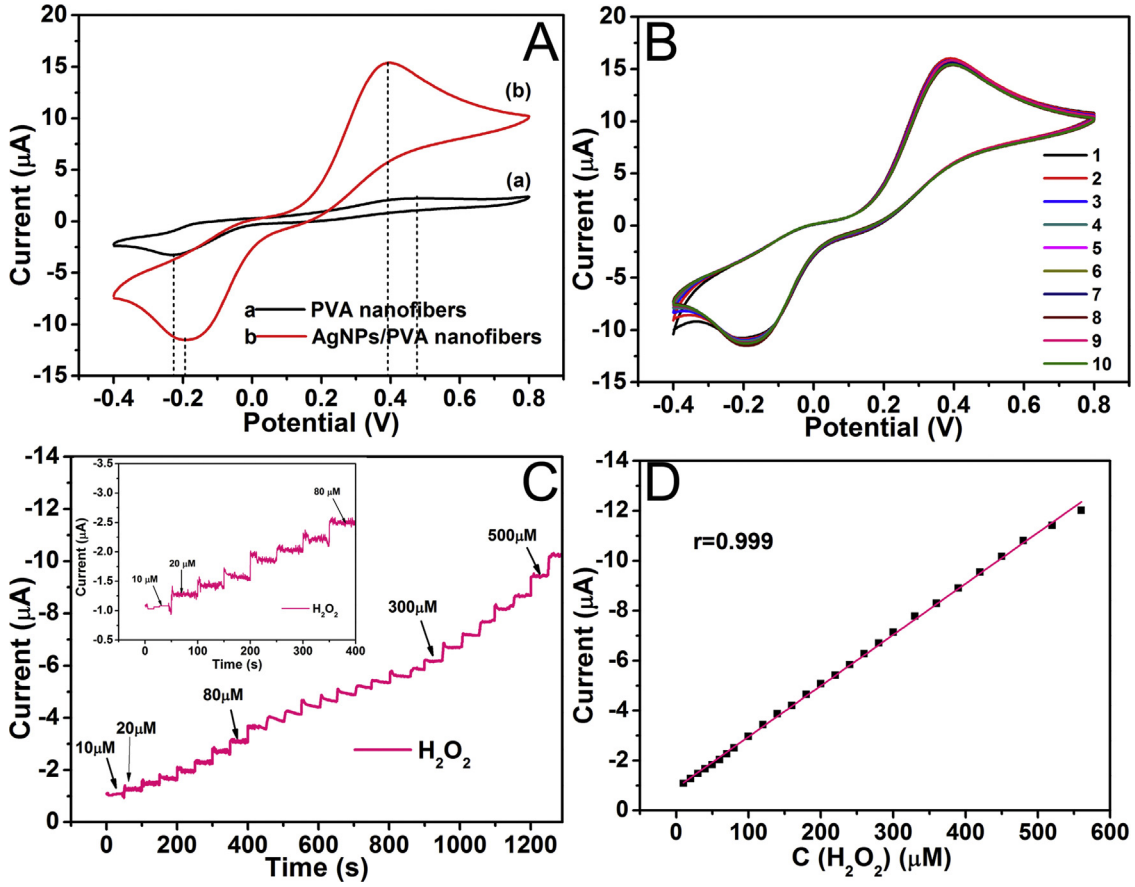

Fig. 12. (A) CVs obtained with AgNPs/PVA and nanofibers functionalized GCE immersed in 1.0 mM HQ in 0.1 M PBS (pH 6.8) in the presence of 5.0 mM H_2O_2 (scan rate, 50 mV s^{-1}); (B) the CVs cycles of the prepared AgNPs/PVA/GCE at the same conditions; (C) amperometric response of the fabricated HRP/(AgNPs/PVA)/GCE biosensor to successive addition of different concentrations of H_2O_2 to 1.0 M phosphate buffer (PB) at −0.19 V. Inset shows the response of the biosensor from 10 μM to 80 μM H_2O_2; (D) relationship of the calibration curve and linear fitting curve between the currents and the H_2O_2 concentration.

excellent stability and reusability of fabricated AgNPs/PVA nanofibers functionalized electrodes. As shown in Fig. 12C and D, a typical current–time response of the sensor with successive additions of H_2O_2 and the calibration plots of the currents versus the concentration of H_2O_2, respectively. The AgNPs/PVA nanofibers biosensor responded rapidly and approached about 98% of its steady state current less than 2 s. The rapid electrode response to the change of the H_2O_2 concentration is attributed to the fast diffusion of the H_2O_2 onto the surface of small AgNPs through the porous nanofibers structures. The linear range spans the concentration of H_2O_2 from 10 μM to 560 μM, with the correlation coefficient of 0.999. The detection limit of 0.56 mM was estimated at a signal-to-noise ratio of 3. The high sensitivity may result in the excellent biocompatible microenvironment of the AgNPs/PVA nanofibers around the enzyme.

4. Conclusion

In summary, a facile and green approach has been demonstrated for the fabrication of highly uniform and mono-disperse NMNPs in PVA nanofibers by combining an in situ reduction and electrospinning technique, which are used as efficient biosensor for the detection of H_2O_2. The small and stable AgNPs, AuNPs and PtNPs with average diameters about 9.4 ± 1.4, 8.0 ± 1.2 and 1.8 ± 0.2 nm, respectively, can be easily obtained in aqueous solution using EGCG as both reductant and stabilizer. Meanwhile, the similar process was used for the preparation of NMNPs/PVA electrospun precursor solution. Through electrospinning technique, uniform and smooth nanofibers can be obtained and the NMNPs with narrow size distributions are well dispersed in PVA nanofibers, which are confirmed by TEM and FE-SEM. UV–vis, FTIR and XPS were used to investigate the growth mechanism of these novel materials. After elaborative studies, it is proposed that the viscosity of the PVA solution play an important role in controlling the size of NMNPs and size-controlled AgNPs are obtained. Based on the large specific area, high conductivity, and good biocompatibility of AgNPs and porosity of the nanofibers, the AgNPs/PVA nanofibers were used as biosensor for the detection of H_2O_2. The fabricated AgNPs/PVA nanofibers functionalized electrodes exhibit remarkable increased electrochemical catalysis toward H_2O_2 and excellent stability and reusability. The fabricated HRP biosensor allowed the highly sensitive detection of H_2O_2 with a broad linear range span of the concentration of H_2O_2 from 10 μM to 560 μM. The rapid electrode response to the change of the H_2O_2 concentration is attributed to the fast diffusion of the H_2O_2 onto the surface of small AgNPs through the porous nanofibers structures. The AgNPs/PVA nanofibrous mats could be further applied to immobilize many other enzymes, and the resulting enzyme/AgNPs/PVA nanofibrous mats may find wide applications in bioelectroanalysis and bioelectrocatalysis.

Acknowledgements

We acknowledge the support of the project of the National Natural Science Foundation of China (NSFC) (Grant number: 51243001), the 521 Project of Zhejiang Sci-Tech University and The Young Researchers Foundation of Key Laboratory of Advanced Textile Materials and Manufacturing Technology, Ministry of Education, Zhejiang Sci-Tech University (Grant number: 2011QN02).

Appendix A. Supplementary data

Supplementary data associated with this article can be found, in the online version, at http://dx.doi.org/10.1016/j.snb.2013.05.062.

References

[1] I. Choi, H.D. Song, S. Lee, Y.I. Yang, T. Kang, J. Yi, Core-satellites assembly of silver nanoparticles on a single gold nanoparticle via metal ion-mediated complex, Journal of the American Chemical Society 134 (2012) 12083–12090.
[2] Y.G. Sun, Y.N. Xia, Shape-controlled synthesis of gold and silver nanoparticles, Science 298 (2002) 2176–2179.
[3] J.E. Millstone, S.J. Hurst, G.S. Metraux, J.I. Cutler, C.A. Mirkin, Colloidal gold and silver triangular nanoprisms, Small 5 (2009) 646–664.
[4] T.K. Sau, A.L. Rogach, Nonspherical noble metal nanoparticles: colloid-chemical synthesis and morphology control, Advanced Materials 22 (2010) 1781–1804.
[5] Y.D. Jin, Engineering plasmonic gold nanostructures and metamaterials for biosensing and nanomedicine, Advanced Materials 24 (2012) 5153–5165.
[6] S. Mao, G.H. Lu, K.H. Yu, Z. Bo, J.H. Chen, Specific protein detection using thermally reduced graphene oxide sheet decorated with gold nanoparticle-antibody conjugates, Advanced Materials 22 (2010) 3521–3526.
[7] J. Lu, I. Do, L.T. Drzal, R.M. Worden, I. Lee, Nanometal-decorated exfoliated graphite nanoplatelet based glucose biosensors with high sensitivity and fast response, ACS Nano 2 (2008) 1825–1832.
[8] N.J. Ronkainen, H.B. Halsall, W.R. Heineman, Electrochemical biosensors, Chemical Society Reviews 39 (2010) 1747–1763.
[9] L.N. Cella, W. Chen, N.V. Myung, A. Mulchandani, Single-walled carbon nanotube-based chemiresistive affinity biosensors for small molecules: ultrasensitive glucose detection, Journal of the American Chemical Society 132 (2010) 5024–5026.
[10] Q. Li, K. Cheng, W.J. Weng, P.Y. Du, G.R. Han, Highly sensitive hydrogen peroxide biosensors based on TiO_2 nanodots/ITO electrodes, Journal of Materials Chemistry 22 (2012) 9019–9026.
[11] Y.H. Sun, R.M. Kong, D.Q. Lu, X.B. Zhang, H.M. Meng, W.H. Tan, G.L. Shen, R.Q. Yu, A nanoscale DNA-Au dendrimer as a signal amplifier for the universal design of functional DNA-based SERS biosensors, Chemical Communications 47 (2011) 3840–3842.
[12] S.Y. Yang, Y.M. Liu, H. Tan, C. Wu, Z.Y. Wu, G.L. Shen, R.Q. Yu, Gold nanoparticle based signal enhancement liquid crystal biosensors for DNA hybridization assays, Chemical Communications 48 (2012) 2861–2863.
[13] C. Wang, H.F. Yin, S. Dai, S.H. Sun, A general approach to noble metal-metal oxide dumbbell nanoparticles and their catalytic application for CO oxidation, Chemistry of Materials 22 (2010) 3277–3282.
[14] A.S. Thakor, J. Jokerst, C. Zavaleta, T.F. Massoud, S.S. Gambhir, Gold nanoparticles: a revival in precious metal administration to patients, Nano Letters 11 (2011) 4029–4036.
[15] Y.N. Xia, Y.J. Xiong, B. Lim, S.E. Skrabalak, Shape-controlled synthesis of metal nanocrystals: simple chemistry meets complex physics? Angewandte Chemie International Edition 47 (2008) 2–46.
[16] M. Roca, A.J. Haes, Silica-void-gold nanoparticles temporally stable surf ace-enhanced Raman scattering substrates, Journal of the American Chemical Society 130 (2008) 14273–14279.
[17] J. Zeng, X.H. Xia, M. Rycenga, P. Henneghan, Q.G. Li, Y.N. Xia, Successive deposition of silver on silver nanoplates: lateral versus vertical growth, Angewandte Chemie International Edition 50 (2011) 244–249.
[18] Y.X. Li, J.T. Cox, B. Zhang, Electrochemical responses and electrocatalysis at single Au nanoparticles, Journal of the American Chemical Society 132 (2010) 3047–3054.
[19] C. Zhu, J. Zeng, J. Tao, M.C. Johnson, I. Schmidt-Krey, L. Blubaugh, Y.M. Zhu, Z.Z. Gu, Y.N. Xia, Kinetically controlled overgrowth of Ag or Au on Pd nanocrystal seeds: from hybrid dimers to nonconcentric and concentric bimetallic nanocrystals, Journal of the American Chemical Society 134 (2012) 15822–15831.
[20] M.R. Langille, M.L. Personick, J. Zhang, C.A. Mirkin, Defining rules for the shape evolution of gold nanoparticles, Journal of the American Chemical Society 134 (2012) 14542–14554.
[21] H. Wu, X. Huang, M.M. Gao, X.P. Lia, B. Shi, Polyphenol-grafted collagen fiber as reductant and stabilizer for one-step synthesis of size-controlled gold nanoparticles and their catalytic application to 4-nitrophenol reduction, Green Chemistry 13 (2011) 651–658.
[22] J. Wang, H.B. Yao, D. He, C.L. Zhang, S.H. Yu, Facile fabrication of gold nanoparticles-poly(vinyl alcohol) electrospun water-stable nanofibrous mats: efficient substrate materials for biosensors, ACS Applied Materials & Interfaces 4 (2012) 1963–1971.
[23] H. Dong, D. Wang, G. Sun, J.P. Hinestroza, Assembly of metal nanoparticles on electrospun nylon 6 nanofibers by control of interfacial hydrogen-bonding interactions, Chemistry of Materials 20 (2008) 6627–6632.
[24] J. Wang, M. Musameh, Y.H. Lin, Solubilization of carbon nanotubes by nafion-toward the preparation of amperometric biosensors, Journal of the American Chemical Society 125 (2003) 2408–2409.
[25] T.J. Zhang, W. Wang, D.Y. Zhang, X.X. Zhang, Y.R. Ma, Y.L. Zhou, L.M. Qi, Biotemplated synthesis of gold nanoparticle-bacteria cellulose nanofiber nanocomposites and their application in biosensing, Advanced Functional Materials 20 (2010) 1152–1160.
[26] N. Chauhan, A. Singh, J. Narang, S. Dahiya, C.S. Pundir, Development of amperometric lysine biosensors based on Au nanoparticles/multiwalled carbon nanotubes/polymers modified Au electrodes, Analyst 137 (2012) 5113–5122.
[27] D. Li, Y.N. Xia, Electrospinning of nanofibers: reinventing the wheels? Advanced Materials 16 (2004) 1151–1170.

[28] D. Li, Y.N. Xia, Electrospinning of polymeric and ceramic nanofibers as uniaxially aligned arrays, Nano Letters 3 (2003) 555–560.
[29] H. Wu, R. Zhang, X.X. Liu, D.D. Lin, W. Pan, Electrospinning of Fe, Co, and Ni nanofibers: synthesis, assembly, and magnetic properties, Chemistry of Materials 19 (2007) 3506–3511.
[30] A.C. Kamps, M. Fryd, S.J. Park, Hierarchical self-assembly of amphiphilic semiconducting polymers into isolated, bundled, and branched nanofibers, ACS Nano 6 (2012) 2844–2852.
[31] H. Zhu, M.L. Du, M.L. Zou, C.S. Xu, N. Li, Y.Q. Fu, Facile and green synthesis of well-dispersed Au nanoparticles in PAN nanofibers by tea polyphenols, Journal of Materials Chemistry 22 (2012) 9301–9307.
[32] H. Zhu, M.L. Du, M.L. Zou, C.S. Xu, Y.Q. Fu, Green synthesis of Au nanoparticles immobilized on halloysite nanotubes for surface-enhanced Raman scattering substrates, Dalton Transactions 41 (2012) 10465–10471.
[33] M.L. Zou, M.L. Du, H. Zhu, C.S. Xu, Y.Q. Fu, Green synthesis of halloysite nanotubes supported Ag nanoparticles for photocatalytic decomposition of methylene Blue, Journal of Physics D: Applied Physics 45 (2012) 325302–325308.
[34] M.L. Zou, M.L. Du, H. Zhu, C.S. Xu, N. Li, Y.Q. Fu, Synthesis of silver nanoparticles in electrospun polyacrylonitrile nanofibers using tea polyphenols as the reductant, Polymer Engineering & Science (2012), DOI 10.1002/pen.23358.
[35] H. Zhu, M.L. Du, D.L. Yu, Y. Wang, L.N. Wang, M.L. Zou, M. Zhang, Y.Q. Fu, A new strategy for the surface-free-energy-distribution induced selective growth and controlled formation of Cu_2O–Au hierarchical heterostructures with a series of morphological evolutions, Journal of Materials Chemistry A 1 (2013) 919–929.
[36] H. Zhu, M.L. Du, D.L. Yu, Y. Wang, M.L. Zou, C.S. Xu, Y.Q. Fu, Selective growth of Au nanograins on specific positions (tips, edges and facets) of Cu_2O octahedrons to form Cu_2O–Au hierarchical heterostructures, Dalton Transactions 41 (2012) 13795–13799.
[37] M.F. Peng, J. Gao, P.P. Zhang, Y. Li, X.H. Sun, S.T. Lee, Reductive self-assembling of Ag nanoparticles on germanium nanowires and their application in ultrasensitive surface-enhanced Raman spectroscopy, Chemistry of Materials 23 (2011) 3296–3301.
[38] R.J. Liao, Z.H. Tang, Y.D. Lei, B.C. Guo, Sodium deoxycholate functionalized graphene and its composites with polyvinyl alcohol, Journal of Physical Chemistry C 115 (2011) 20740–20746.
[39] X. Huang, H. Wu, X.P. Liao, B. Shi, One-step, size-controlled synthesis of gold nanoparticles at room temperature using plant tannin, Green Chemistry 12 (2010) 395–399.
[40] A.S. Asran, K. Razghandi, N. Aggarwal, G.H. Michler, T. Groth, Nanofibers from blends of polyvinyl alcohol and polyhydroxy butyrate as potential scaffold material for tissue engineering of skin, Biomacromolecules 11 (2010) 3413–3421.
[41] Y.P. Huang, H. Ma, S.G. Wang, M.W. Shen, R. Guo, X.Y. Cao, M.F. Zhu, X.Y. Shi, Efficient catalytic reduction of hexavalent chromium using palladium nanoparticle-immobilized electrospun polymer nanofibers, ACS Applied Materials & Interfaces 4 (2012) 3054–3061.
[42] Y. Ding, Y. Wang, L. Su, H. Zhang, Y. Lei, Preparation and characterization of NiO-Ag nanofibers, NiO nanofibers, and porous Ag: towards the development of a highly sensitive and selective non-enzymatic glucose sensor, Journal of Materials Chemistry 20 (2010) 9918–9926.
[43] P.R. Selvakannan, A. Swami, D. Srisathiyanarayanan, P.S. Shirude, R. Pasricha, A.B. Mandale, M. Sastry, Synthesis of aqueous Au core-Ag shell nanoparticles using tyrosine as a pH-dependent reducing agent and assembling phase-transferred silver nanoparticles at the air–water interface, Langmuir 20 (2004) 7825–7836.
[44] P. Jiang, S.Y. Li, S.S. Xie, Y. Gao, L. Song, Double-stranded helices and molecular zippers assembled from single-stranded coordination polymers directed by supramolecular interactions, Chemistry - A European Journal 10 (2004) 4817–4821.
[45] X.M. Feng, R.M. Li, Y.W. Ma, R.F. Chen, N.E. Shi, Q.L. Fan, W. Huang, One-step electrochemical synthesis of graphene/polyaniline composite film and its applications, Advanced Functional Materials 21 (2011) 2989–2996.
[46] X. Zhong, R. Yuan, Y.Q. Chai, In situ spontaneous reduction synthesis of spherical Pd@Cys-C-60 nanoparticles and its application in nonenzymatic glucose biosensors, Chemical Communications 48 (2012) 597–599.
[47] Y. Li, J.J. Zhang, J. Xuan, L.P. Jiang, J.J. Zhu, Fabrication of a novel nonenzymatic hydrogen peroxide sensor based on Se/Pt nanocomposites, Electrochemistry Communications 12 (2010) 777–780.
[48] H. Zhu, M.L. Du, M. Zhang, P. Wang, S.Y. Bao, L.N. Wang, Y.Q. Fu, J.M. Yao, Facile fabrication of AgNPs/(PVA/PEI) nanofibers: high electrochemical efficiency and durability for biosensors, Biosensors and Bioelectronics (2013), http://dx.doi.org/10.1016/j.bios.2013.04.016.
[49] S. Myung, A. Solanki, C.J. Kim, J. Park, K.S. Kim, K.B. Lee, Graphene-encapsulated nanoparticle-based biosensor for the selective detection of cancer biomarkers, Advanced Materials 23 (2011) 2221–2225.
[50] I.M. Feigel, H. Vedala, A. Star, Biosensors based on one-dimensional nanostructures, Journal of Materials Chemistry 21 (2011) 8940–8954.
[51] O. Akhavan, E. Ghaderi, Copper oxide nanoflakes as highly sensitive and fast response self-sterilizing biosensors, Journal of Materials Chemistry 21 (2011) 12935–12940.
[52] Y. Ding, Y. Wang, L.C. Zhang, H. Zhang, C.M. Li, Y. Lei, Preparation of TiO_2-Pt hybrid nanofibers and their application for sensitive hydrazine detection, Nanoscale 3 (2011) 1149–1157.

Biographies

Han Zhu received his from bachelor's degree in 2011 from NanJing University of Technology. He is a PhD candidate in materials science in Zhejiang Sci-Tech University. His research areas include nanomaterials, electrospinning and biosensors.

MingLiang Du received his PhD in materials science and engineering from South China University of Technology in 2007. He is now an associate professor in faculty of Materials and Textiles in the Zhejiang Sci-Tech University. His research interests are in field of polymer functional materials and nanomaterials.

Ming Zhang obtained her PhD in 2005 from Jilin University, and joined Professor ZhongFan Liu's group as a postdoctoral fellow at Peking University in 2005. She is now worked in faculty of Materials and Textiles in the ZheJiang Sci-Tech University. Her research interests are in field of miniemulsion polymerization.

Pan Wang received her bachelor's degree in 2012 from Zhong Yuan University of Technology. She is a graduate student in materials science in ZheJiang Sci-Tech University. Her research areas include nanomaterials and electrospinning.

Shiyong Bao received his bachelor's degree in 2012 from ZheJiang Sci-Tech University. He is a graduate student in materials science in ZheJiang Sci-Tech University. His research areas include nanomaterials and electrospinning.

Yaqin Fu received her PhD degree from Kyoto institute of technology in 2004. She is now a professor in Faculty of Materials and Textiles in ZheJiang Sci-Tech University. Her research interests are in field of the functional fiber and composite materials.

Ju ming Yao received his PhD degree in 2003 from Tokyo University of Agriculture and Technology. He is now a professor and doctoral supervisor in faculty of Materials and Textiles in ZheJiang Sci-Tech University. His research interests are in field of biopolymer materials.